Energy spectrum in the inertial and dissipation ranges of two-dimensional steady turbulence

Toshiyuki Gotoh
Department of System Engineering, Nagoya Institute of Technology, Showa-ku, 466, Nagoya, Japan
(Received 27 March 1997; revised manuscript received 27 October 1997)

The energy spectrum in the inertial and dissipation ranges in two-dimensional steady turbulence is examined theoretically and by high resolution direct numerical simulations (DNS) up to $N=4096^2$. A theoretical spectrum smoothly joining the two ranges is derived using the Kármán-Howarth-type equation. In the inertial range we obtain an asymptotic form of the energy spectrum as $E(k)=C\eta^{2/3}k^{-3}(k/k_d)^{-\delta}[\ln(k/k_I)]^{-(2-\delta)/(6-\delta)}$ with small δ. It is found from the DNS that δ decreases slowly with the microscale Reynolds number and the constant C is of the order of unity but increases with the microscale Reynolds number. In the far dissipation range, we derive $E(k)\propto k^{-(3+\delta)/2}e^{-\alpha_2(k/k_d)}$, which agrees with the DNS results. The slope α_2 depends explicitly on the microscale Reynolds number and agrees with the DNS values. Universality of the spectrum in the two ranges is also discussed. [S1063-651X(98)10703-1]

PACS number(s): 47.27.Gs, 47.27.Jv, 47.27.Ak

I. INTRODUCTION

The energy spectrum is the quantity of central interest in the study of turbulence. Recent high performance computers enable us to simulate two-dimensional turbulence with very high resolution [1–12]. Most of the studies using direct numerical simulation (DNS) have been concerned with decaying turbulence, in which long lived coherent vortices emerge and are strongly dependent on initial conditions. In this case, one is unlikely to see universality in the satistics of the turbulence. On the other hand, in the case of steady two-dimensional turbulence excited by pumping of vorticity with a macroscale $1/k_I$, it is commonly seen that irrespective of forcing mechanisms, self-similar, very thin vortex layers develop in between vortices having the forcing scale. The inertial range spectrum predicted by theory [15–17] is of the form of $E(k)\propto k^{-3}$ or log-corrected one,

$$E_\infty(k)\propto \eta^{2/3}k^{-3}[\ln(k/k_I)]^{-1/3}, \tag{1}$$

by Kraichnan [18], where $\eta^{2/3}$ is the average rate of the enstrophy dissipation. The energy spectrum in the enstrophy cascading range by the DNS has been observed to be $k^{-(3+\delta)}$ with $0<\delta<1$ for normal viscosity [3,10–12] and to tend to be $k^{-3}[\ln(k/k_I)]^{-1/3}$ for hyperviscosity [10].

It still is an open question what the form of the energy spectrum is in the inertial-to-far dissipation ranges at large but finite Reynolds numbers. What we need to know is the statistics of two-dimensional turbulence with normal viscosity, and the energy spectrum is fundamental. Most high resolution DNS's use hyperviscosity in order to obtain wider inertial range than in the case of normal viscosity. However, using hyperviscosity changes completely the statistics of the scales of motion in the range of inertial to dissipation, and would affect the higher order moments, which may not be independent of the viscosity, as shown in recent studies of a passive scalar convected by a random velocity field [13,14].

For finite Reynolds number, as we see in the latter sections, the spectrum where the inerial effect is dominant is approximately algebraic, while for infinite Reynolds number it is of log-corrected form, Eq. (1). It is not known how the former spectrum approaches the latter in the asymptotic limit. Also, less attention has been paid to the form of the spectrum in the dissipation range. For decaying turbulence, Tatsumi and Yanase [25] studied an analytical form of the spectrum in this range using the Modified Zero-4th theory. The form is

$$E(k)\propto k^{5/2}\exp[-\alpha_2(k/k_d)], \tag{2}$$

$$\alpha_2(\tau)=b\tau^{1/2}[\ln(R_L\tau)]^{-1/6}, \tag{3}$$

where b is a constant of the order of unity, $R_L=u_0/\nu k_I$ is the macroscale Reynolds, number and $\tau=u_0k_It$ is nondimensional time. But no studies have been done for steady turbulence.

In this paper we present a simple analysis of the energy spectrum that smoothly joins the inertial and dissipation ranges for normal viscosity, and compare with DNS results of steady turbulences of high resolution up to $N=4096^2$ [11,12].

II. ANALYSIS OF THE ENERGY SPECTRUM

The equation for the second-order moment of vorticity difference $Q_2(\boldsymbol{r},t)=\langle(\omega(\boldsymbol{x}+\boldsymbol{r},t)-\omega(\boldsymbol{x},t))^2\rangle$ is given by

$$\frac{\partial Q_2(\boldsymbol{r},t)}{\partial t}+\frac{\partial Q_{3i}(\boldsymbol{r},t)}{\partial r_i}=-4\eta+2\nu\nabla^2Q_2(\boldsymbol{r},t), \tag{4}$$

where $\eta=\nu\langle(\partial\omega/\partial x_I)^2\rangle$ is the average rate of enstrophy dissipation per unit mass, $Q_{3i}(\boldsymbol{r})=\langle\delta u_i(\boldsymbol{r})[\delta\omega(\boldsymbol{r})]^2\rangle$ and $\delta u_i=u_i(\boldsymbol{x}+\boldsymbol{r})-u_i(\boldsymbol{x})$. Since for $|\boldsymbol{r}|=r\ll 1/k_I$, the turbulence field is homogeneous, isotropic and in a quasi-steady-state, we put $\partial Q_2/\partial t=0$ and $Q_{3i}(\boldsymbol{r})=Q_3(r)r_i/r$ where $Q_3(r)$ is a nondimensional function. Substituting this expression into Eq. (4) and integrating with respect to r we obtain

$$Q_3(r)=-2\eta r+2\nu\frac{dQ_2(r)}{dr}. \tag{5}$$

In the inertial range $r\gg l_d=(\nu^3/\eta)^{1/6}=1/k_d$, the viscosity term can be neglected; then Eq. (5) becomes

$$Q_{3i}(\boldsymbol{r})r_i/r=-2\eta r, \tag{6}$$

which is a two-dimensional analogue of Kolmorogov's 4/5 law in three-dimensional turbulence.

When r is in the dissipation range, we must retain the viscosity term. Multiplying Eq. (5) by r_1/r we have the equation projected onto a one-dimensional axis as

$$Q_{31}(x)=-2\eta x+2\nu\frac{dQ_2}{dx}. \tag{7}$$

For $x\ll l_d$, we can write

$$\lim_{x\to 0}\frac{Q_{31}(x)}{x^3}=-\frac{S_2}{8}\frac{\eta}{\nu}\Omega^{1/2}+O(x^2), \tag{8}$$

where S_2 is the two-dimensional skewness

$$S_2=-2\frac{\left\langle \frac{\partial u_1}{\partial x}\left(\frac{\partial\omega}{\partial x}\right)^2\right\rangle}{\left\langle\left(\frac{\partial u_1}{\partial x}\right)^2\right\rangle^{1/2}\left\langle\left(\frac{\partial\omega}{\partial x}\right)^2\right\rangle} \tag{9}$$

and Ω is the total enstrophy defined by

$$\Omega=\tfrac{1}{2}\langle\omega^2\rangle. \tag{10}$$

It should be noted that closure of the third order moment is made by using the two-dimensional skewness S_2, which is the product of the velocity gradient and the vorticity gradient. Substituting Eq. (8) into Eq. (7), integrating over x and using the Padé approximation we have

$$F(\tilde{x})\equiv 2\eta^{-2/3}Q_2(\tilde{x})=\tilde{x}^2-\frac{S_2}{32}\mathcal{R}_\lambda^{1/3}\tilde{x}^4+O(\tilde{x}^6)\approx\frac{a^2\tilde{x}^2}{a^2+\tilde{x}^2}, \tag{11}$$

$$a^2=32/(S_2\mathcal{R}_\lambda^{1/3}) \tag{12}$$

for $\tilde{x}=xk_d\ll 1$, where

$$\mathcal{R}_\lambda\equiv\frac{\Omega^{3/2}}{\eta} \tag{13}$$

is the microscale Reynolds number [19].

In the inertial range we assume tentatively that the energy spectrum is of the form

$$E(k)=C'\eta^{2/3}k^{-3}\left(\frac{k}{k_d}\right)^{-\delta} \tag{14}$$

with $\delta\geqslant 0$, which means $Q_2(x)\sim\eta^{2/3}x^\delta$ and

$$F(\tilde{x})\sim\tilde{x}^\delta,\quad \tilde{x}\gg 1. \tag{15}$$

A smooth function that matches both Eqs. (11) and (15) is

$$F(\tilde{x})=\frac{\tilde{x}^2}{[1+(\tilde{x}/b)^2]^{(2-\delta)/2}},\quad b^2=\frac{16(2-\delta)}{S_2\mathcal{R}_\lambda^{1/3}}, \tag{16}$$

where b is the scale at which the inertial and dissipation ranges cross over. This may be compared with the formula in three-dimensional turbulence,

$$\frac{15}{(\overline{\epsilon}\nu)^{1/2}}Q_2(\tilde{x})\approx\frac{\tilde{x}^2}{[1+(\tilde{x}/c)^2]^{2/3}},$$

$$c^2=\frac{8}{S_3}\frac{15^{3/2}}{5},\quad S_3=\frac{\left\langle\left(\frac{\partial u}{\partial x}\right)^3\right\rangle}{\left\langle\left(\frac{\partial u}{\partial x}\right)^2\right\rangle^{3/2}} \tag{17}$$

studied by Batchelor [20], where S_3 is the three-dimensional skewness, $\tilde{x}=x/l_{d3}$ and $l_{d3}=(\nu^3/\overline{\epsilon})^{1/4}$ is the Kolmogorov length (for more elaborate expressions with or without intermittency correction, see Refs. [21,22]).

The one-dimensional correlation function for the vorticity is given by

$$W_1(\tilde{x})\equiv\langle\omega(\boldsymbol{x}+\tilde{x})\omega(\boldsymbol{x})\rangle/\langle\omega^2\rangle=1-\frac{1}{8\mathcal{R}_\lambda^{2/3}}F(\tilde{x}), \tag{18}$$

and the corresponding one-dimensional spectrum can be written as

$$W_1(\tilde{k})=\frac{1}{2\pi}\int_{-\infty}^{\infty}W_1(\tilde{x})e^{-i\tilde{k}\tilde{x}}d\tilde{x}$$

$$=A\frac{\partial^2}{\partial\tilde{k}^2}\left[\left(\frac{\tilde{k}}{2b}\right)^\sigma K_\sigma(b\tilde{k})\right],$$

$$A=\frac{b^{2-\delta}}{8\pi^{1/2}\Gamma(\sigma+1/2)\mathcal{R}_\lambda^{2/3}},\quad \tilde{k}=kl_d,\quad \sigma=\frac{1-\delta}{2}, \tag{19}$$

where $K_\mu(z)$ is the modified Bessel function of the order μ. The energy spectrum $E(k)$, then, is given by [23]

$$\overline{E(\tilde{k})}\equiv E(k)k_d^3/\Omega=\frac{Ab^{1-\sigma}}{2^\sigma}\tilde{k}^{-3}\int_{\tilde{k}}^{\infty}\{[b^2z^2+4\sigma(\sigma-1)$$

$$+1]K_{\sigma-1}(bz)-2\sigma bzK_\sigma(bz)\}\frac{z^\sigma}{\sqrt{z^2-\tilde{k}^2}}dz. \tag{20}$$

The asymptotic form of the spectrum is

$$\overline{E(\tilde{k})}\propto\tilde{k}^{-(3+\delta)},\quad \text{for}\quad \tilde{k}\ll 1,$$

$$\propto\tilde{k}^{-(3+\delta)/2}e^{-\alpha_2\tilde{k}},\quad \text{for}\quad \tilde{k}\gg 1. \tag{21}$$

In the inertial range $E(k)$ is proportional to $k^{-(3+\delta)}$, while in the dissipation range it decays exponentially at a rate α_2. It should be noted that the exponent of the prefactor in the dissipation range is $-(3+\delta)/2$, half of the exponent in the inertial range. This can be compared with the results, $E(k)\propto k^{-3}$ in the inertial range and $\propto k^3\exp[-\alpha_2(k/k_d)]$ in the dis-

sipation range by the statistical theories of turbulence such as the direct interaction approximation (DIA) [24], Modified Zero-4th [25], and Lagrangian renormalized approximation (LRA) [26]. There, the exponent of the prefactor is 3, which is different from $-(3+\delta)/2$ as found in Eq. (21). The exponential decay is the same.

We obtain α_2 as

$$\alpha_2=\left(\frac{16(2-\delta)}{S_2}\right)^{1/2}\mathcal{R}_\lambda^{-1/6}, \tag{22}$$

which may be compared to Eq. (3) for decaying turbulence. Equation (3) depends on the macroscale Reynolds number, while Eq. (22) depends on the microscale Reynolds number $\mathcal{R}_\lambda$. The decay rate α_2 depends explicitly on $\mathcal{R}_\lambda^{-1/6}$, which arises from the normalization factor of S_2, whose dependence on $\mathcal{R}_\lambda$ is very weak.

In three dimensional turbulence, on the other hand, the decay rate α_3 of the energy spectrum in the dissipation range, where $E(k)\propto\exp[-\alpha_3(k/k_d)]$, is given by $\alpha_3=(16\sqrt{15}/S_3)^{1/2}$, which has no explicit dependence on $\mathcal{R}_{\lambda_{3d}}$ [22,27]. If, therefore, the skewness S_3 does not depend on $\mathcal{R}_{\lambda_{3d}}$ in three dimensions (although it actually depends on $\mathcal{R}_{\lambda_{3d}}$ very weakly), the energy spectrum in the dissipation range is independent of $\mathcal{R}_{\lambda_{3d}}$. The difference is due to the fact that in three dimensions the third order moment appearing in the Kármán-Howarth equation contains only the velocity difference as $Q_{3i}^{3D}(\boldsymbol{r})=\langle\delta u_i(\boldsymbol{r})[\delta u(\boldsymbol{r})]^2\rangle$, while in two dimensions $Q_{3i}(\boldsymbol{r})=\langle\delta u_i(\boldsymbol{r})[\delta\omega(\boldsymbol{r})]^2\rangle$ contains velocity and vorticity differences. In other words, $Q_{3i}(\boldsymbol{r})$ has contributions from two ranges of wave numbers, near k_I and k_d. This affects the closure of the third order moment using the skewness S_2 in the far dissipation range, so that $\mathcal{R}_\lambda^{-1/6}$ dependency appears.

III. COMPARISON WITH THE DNS

Let us compare our results with the DNS results [11,12]. The vorticity equation integrated using the pseudospectral method is

$$\frac{\partial\omega}{\partial t}+\frac{\partial(\psi,\omega)}{\partial(x,y)}=\nu\nabla^2\omega+\nu'\nabla^{-2}\omega+f(\boldsymbol{x},t), \tag{23}$$

$$\nabla^2\psi=-\omega, \tag{24}$$

$$\langle f(\boldsymbol{x},t)f(\boldsymbol{x}',s)\rangle=F(\boldsymbol{x}-\boldsymbol{x}')\delta(t-s), \tag{25}$$

where ν' is introduced to shut down the inverse cascade of the energy to low wave numbers, and set to be 2 for $k\leqslant 3$ and zero otherwise. The random force $f(\boldsymbol{x},t)$ is Gaussian white and its spectrum support $E_F(k)$ is limited to the band $4\leqslant k\leqslant 6$ and normalized as $F(0)=10^3\Delta t$. The total energy is defined by

$$E=\frac{\langle\boldsymbol{u}^2\rangle}{2}=u_L^2, \tag{26}$$

where u_L is the root mean square of the one-dimensional component of the velocity vector. The integral scale and microscale are defined by

TABLE I. DNS parameters. N, resolution; $k_{\max}$, maximum wave number; ν, kinematic viscosity; δ, the exponent defined by Eq. (14).

	run1	run2	run3	run4
N	1024^2	2048^2	4096^2	4096^2
$k_{\max}$	483	965	1931	1931
ν	1.0×10^{-4}	2.0×10^{-5}	7.0×10^{-6}	3.0×10^{-6}
Δt	5.86×10^{-4}	2.93×10^{-4}	7.32×10^{-4}	1.47×10^{-4}
R_L	2.3×10^3	1.4×10^4	4.1×10^4	9.2×10^4
$\mathcal{R}_\lambda$	23	40	59	67
$\langle\mathbf{u}\rangle^2/2$	0.170	0.171	0.157	0.142
Ω	4.36	4.63	4.50	4.35
$1/k_I$	0.660	0.729	0.744	0.733
λ	3.32×10^{-2}	1.94×10^{-2}	1.40×10^{-2}	9.78×10^{-3}
k_d	85.7	177	279	414
η	0.40	0.25	0.16	0.136
S_2	0.700	0.723	0.730	0.673
δ	0.509	0.430	0.374	0.355
α_2	3.463	3.181	3.023	3.11
C	0.825	1.07	1.39	1.46
C'	0.596	0.726	0.893	0.931

$$L=1/k_I\equiv\frac{u_L}{\eta^{1/3}},\quad \lambda\equiv\left(\frac{\nu\Omega}{\eta}\right)^{1/2}, \tag{27}$$

respectively, and the integral-scale Reynolds number is

$$R_L=\frac{u_L L}{\nu}=\frac{\langle\boldsymbol{u}^2\rangle}{2\nu\eta^{1/3}}. \tag{28}$$

In the second equality of Eq. (28), an estimate for η,

$$\eta\sim\frac{u_L\Omega}{L}, \tag{29}$$

is used. The details of numerical parameters are listed in Table I. Note that the integral-scale Reynolds number R_L is very large while the microscale Reynolds number $\mathcal{R}_\lambda$ is moderate and varies slowly against R_L. The Reynolds number in the usual sense is given by R_L and $\mathcal{R}_\lambda$ is introduced to characterize the inertial effect at small scales.

Figure 1 shows the time averaged energy spectra for four $\mathcal{R}_\lambda$'s, which are multiplied by $k^{3+\delta}$ in order to show the plateau over a range of wave numbers. In that range we observed also that the enstrophy flux $\Pi(k)$ was nearly constant. Values of δ in Fig. 2 are determined by least square fit for several choices of wave-number ranges for a given $\mathcal{R}_\lambda$. It is found that the value of δ satisfies the upper bound $\delta<2/3$ derived from Hölder's inequality [28] and lower than 4/7 derived by Polyakov [29]. The value of δ decreases roughly as $\mathcal{R}_\lambda^{-1/3}$, although it is difficult to definitely determine the slope due to the fluctuations of δ.

Figure 3 shows the compensated spectra $k^{(3+\delta)/2}E(k)$ in the dissipation range. The slope of the spectrum was determined by least square fit over the range of wave numbers of $1\leqslant k/k_d\leqslant 4$. We observe that the compensation of the prefactor $k^{-(3+\delta)/2}$ is crucial to obtain long linear portions of the

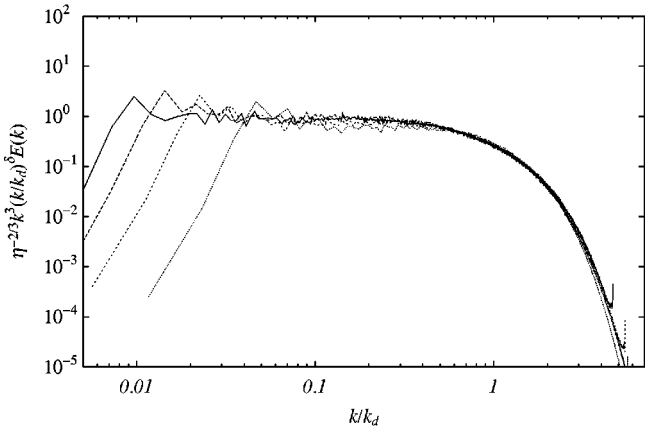

FIG. 1. Scaled energy spectra, $k^{3+\delta}E(k)/\eta^{2/3}$ in the inertial range. Solid line, $\mathcal{R}_\lambda=67$; dashed line, $\mathcal{R}_\lambda=59$; dotted line, $\mathcal{R}_\lambda=40$; fine dotted line, $\mathcal{R}_\lambda=23$.

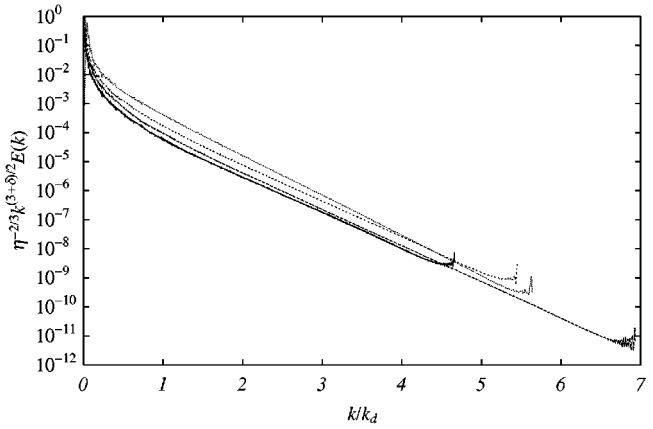

FIG. 3. Scaled energy spectra $k^{(3+\delta)/2}E(k)/\eta^{2/3}$ in the dissipation range. Solid line, $\mathcal{R}_\lambda=67$; dashed line, $\mathcal{R}_\lambda=59$; dotted line, $\mathcal{R}_\lambda=40$; fine dotted line, $\mathcal{R}_\lambda=23$.

spectra in the far dissipation range. When $k^{3+\delta}E(k)$ was plotted against k/k_d, the curves appeared to be convex upward and would wrongly be read as $E(k)\propto \exp[-\alpha_2'(k/k_d)^\gamma]$, $\gamma>1$ as the width of the far dissipation range is not enough. We thus conclude that the prefactor is of the form of $k^{-(3+\delta)/2}$ in the dissipation range.

Variation of the skewness S_2 with $\mathcal{R}_\lambda$ is shown in Fig. 2 and appears to be very insensitive to $\mathcal{R}_\lambda$ as in the case of S_3 in three dimensions. This means that the slope α_2 varies as $\mathcal{R}_\lambda^{-1/6}$. Figure 4 shows the comparison of the slope observed in the DNS with α_2, Eq. (22) using the measured value of δ of the DNS. Agreement is satisfactory, but the slope by the theory is slightly larger than the DNS values.

IV. THE LIMIT OF SMALL δ

When the viscosity is sufficiently small, we expect that δ is very small and the energy spectrum in the inertial range tends to Eq. (1). However, Eq. (14) does not. It is interesting to see how the energy spectrum approaches the log-corrected one as δ vanishes. For this purpose, it is useful to briefly review the process of deriving Eq. (1). That is, for very small viscosity, the strain acting on the scale $1/k$ denoted by

$$\Omega_k=\omega_k^2=\int_{k_I}^{k}p^2E(p)dp \tag{30}$$

must be finite and the logarithm of the wave-number ratio k/k_I comes from the integral of Ω_k. In the inertial range, the enstrophy transfer rate

$$\Lambda(k)\sim\omega_k k^3E(k) \tag{31}$$

is independent of the wave number and equal to η, so that the exponent $-1/3$ of Eq. (1) is obtained.

When Eq. (14) is substituted into Eq. (30), the width of the wave number range contributing to Ω_k increases with decreasing δ and the integral is asymptotically close to $\ln(k/k_I)$. It then follows that $E(k)$ must contain a factor of $\ln(k/k_I)$ for $\Lambda(k)$ to be independent of the wave number. Now we assume that the energy spectrum in the inertial range is of the form

$$E(k)=C\eta^{2/3}k^{-3}\left(\frac{k}{k_d}\right)^{-\delta}\left[\ln\left(\frac{k}{k_I}\right)\right]^{-\beta}, \tag{32}$$

where β is assumed to be a function of δ. When this is substituted into Eqs. (30) and (31), we obtain

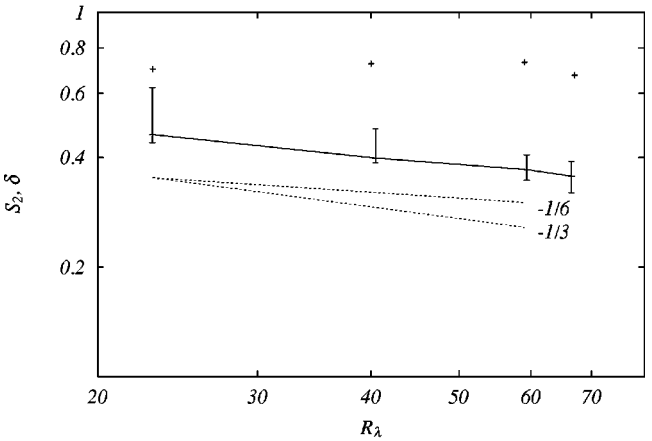

FIG. 2. Variation of δ (solid line with error bar) and skewness (plus) with $\mathcal{R}_\lambda$. Dotted lines show the slopes 1/3 and 1/6.

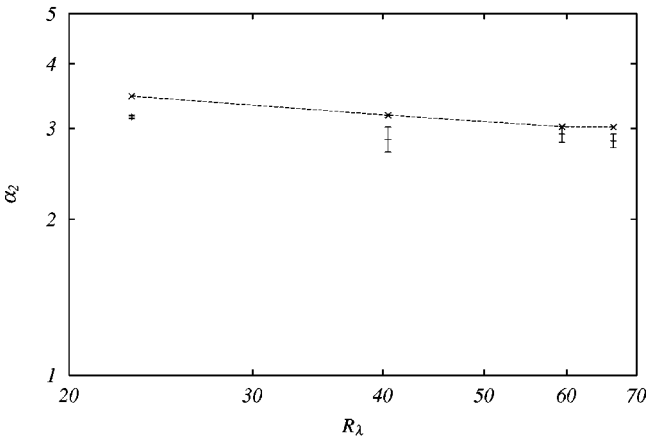

FIG. 4. Comparison of α_2. Dashed line, theory; symbols with error bar, DNS.

$$\Omega_k \sim \frac{C}{1-\beta}\eta^{2/3}\left(\frac{k}{k_d}\right)^{-\delta}[\ln(k/k_I)]^{1-\beta}, \tag{33}$$

$$\Lambda(k) \sim \frac{C^{3/2}}{\sqrt{1-\beta}}\eta\left(\frac{k}{k_d}\right)^{-3\delta/2}[\ln(k/k_I)]^{(1-3\beta)/2}. \tag{34}$$

Since $\Lambda(k)$ is very weakly dependent on the wave number when δ is small but finite, the ''inertial range'' referred to previously should be understood as a quasi-inertial range. The total enstrophy Ω is roughly approximated by putting $k=k_d$ for Ω_k, so that for small δ, $\mathcal{R}_\lambda$ is approximately

$$\mathcal{R}_\lambda \sim \left(\frac{C}{1-\beta}\right)^{3/2}[\ln(k_d/k_I)]^{3(1-\beta)/2}. \tag{35}$$

The matching conditions for the function $F(\tilde{x})$ in the case of the energy spectrum Eq. (32) are given by

$$F(\tilde{x}) \sim \tilde{x}^{\delta}\left[\ln\left(\frac{k_d}{k_I\tilde{x}}\right)\right]^{-\beta}, \tag{36}$$

for large $\tilde{x}$ (for details of calculation see the Appendix), and

$$F(\tilde{x}) \approx \tilde{x}^2 - \frac{S_2}{32}\left(\frac{C}{1-\beta}\right)^{1/2}[\ln(k_d/k_I)]^{(1-\beta)/2}\tilde{x}^4 + O(\tilde{x}^6), \tag{37}$$

for small $\tilde{x}$, where $\mathcal{R}_\lambda^{1/3}$ in Eq. (11) is replaced by the approximation Eq. (35) for the argument below. Then a smooth function $F(\tilde{x})$ satisfying the matching conditions is given by the equation

$$F(\tilde{x}) = \frac{\tilde{x}^2}{[1+(\tilde{x}/b(\tilde{x}))^2]^{(2-\delta)/2}}, \tag{38}$$

with a slowly varying function $b(\tilde{x})$ instead of the constant b; that is,

$$b^2(\tilde{x}) = \left[\ln\left(\frac{k_d}{k_I\tilde{x}}\right)\right]^{-[2\beta/(2-\delta)]}, \quad \text{for} \quad \tilde{x} \gg 1,$$

$$\approx \frac{16(2-\delta)}{S_2}\left(\frac{C}{1-\beta}\right)^{-1/2}[\ln(k_d/k_I)]^{-(1-\beta)/2} \tag{39}$$

$$\text{for} \quad \tilde{x} \ll 1. \tag{40}$$

If we assume that Eq. (36) and Eq. (40) can be extrapolated to $\tilde{x} \sim 1$, respectively, and match each other, the exponent must satisfy the relation $-2\beta/(2-\delta) = -(1-\beta)/2$ for $\tilde{x} \sim 1$, so that we have

$$\beta = \frac{2-\delta}{6-\delta}. \tag{41}$$

When δ tends to zero, β approaches 1/3 and $\Lambda(k)$ becomes independent of the wave number. In fact, we observe in Fig. 5 that the compensated spectra using Eqs. (32) and (41) has a slightly wider plateau than the one by Eq. (14). The constants C' and C in the inertial range spectrum from the DNS are of the order of unity but increase slowly with $\mathcal{R}_\lambda$ (see Fig. 6). The values of C are consistent with the values of 2.626 by the test field model (TFM) [18] and 1.44 by the LRA [30]. The functional form of the slope α_2 by Eq. (22) is unchanged. When the formula Eq. (32) is used, the values for δ and α_2 become smaller than those in Table I by about 10% and 5%, respectively.

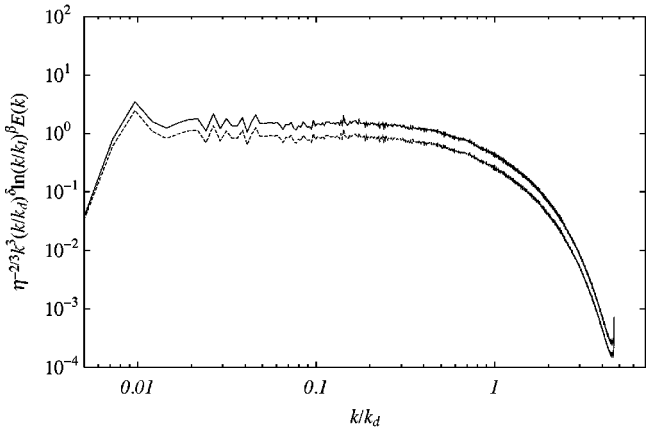

FIG. 5. Comparison of the energy spectra by DNS. $\mathcal{R}_\lambda = 67$. Solid line, $\eta^{-2/3}k^3(k/k_d)^{-\delta}[\ln(k/k_I)]^{-\beta}E(k)$; dashed line, $\eta^{-2/3}k^3(k/k_d)^{-\delta}E(k)$.

For relatively large $\delta \sim 1$, on the other hand, $\beta = 1/5$, a smaller exponent of the logarithmic factor than 1/3, which means that the energy spectrum becomes $E(k) \propto k^{-4}[\ln(k/k_I)]^{-1/5}$ and is consistent with the observation of the energy spectrum in the DNS at low to moderate Reynolds numbers.

V. SUMMARY AND DISCUSSION

We analyzed the energy spectrum using a Kármán-Howarth-type equation and compared it with the results of high resolution DNS. The analysis yielded the spectrum in the inertial-to-far dissipation ranges at large but finite Reynolds numbers. It was shown that the inertial range energy spectrum is of the form given by Eq. (32) and the exponent

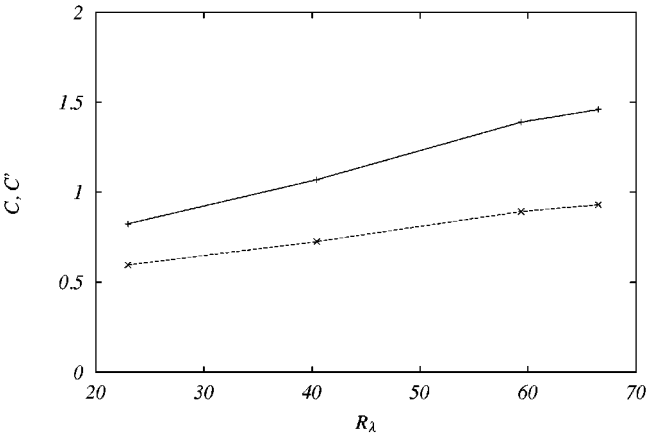

FIG. 6. Variation of the constants C and C' with $\mathcal{R}_\lambda$. Solid line, C; dashed line, C'.

$\beta(\delta)$ of the correction $[\ln(k/k_I)]^{-\beta(\delta)}$ approaches 1/3 as δ vanishes, that is, Kraichnan's spectrum, Eq. (1), is recovered for infinite Reynolds number. It was found from the DNS data that δ decreases as $\mathcal{R}_\lambda$ increases. The constant C of the inertial range spectrum was also measured by the DNS and found to be of the order of unity and to increase with the Reynolds number. In the dissipation range, the exponent of the prefactor in the spectrum is half that in the inertial range. The exponential decay rate of the energy spectrum in the dissipation range is dependent on $\mathcal{R}_\lambda$ and δ for finite Reynolds numbers.

In the above discussion, no effects of forcing have been taken into account. If they are included, a term $-(2/r)\int_0^r r' F(r')dr'$ is added to the right-hand side of Eq. (5). When the spectrum support of the forcing centered on k_I is narrow as in our DNS, then this yields the contribution $-\eta k_I^2 \tilde{x}^4/4$ and gives the slope $\alpha_2' = \alpha_2(1 - 4(k_I/k_d)^2/(S_2\mathcal{R}_\lambda^{1/3}))$. Thus we conclude that the correction for the forcing with narrow spectrum support near k_I is negligible as long as $k_I \ll k_d$.

Also not included in the analysis are the intermittency effects of the vorticity field. If these effects were included, they would appear predominantly as fluctuations of k_d due to the spatial variation of $\eta(\boldsymbol{x})$ [24]. Locally defined $k_d(\boldsymbol{x}) = [\eta(\boldsymbol{x})/\nu^3]^{1/6}$ fluctuates in space so that regions having a large amplitude of $\eta(\boldsymbol{x})$ dominating the energy spectrum in the far dissipation range because $E(k,\boldsymbol{x}) \propto \exp\{-\alpha_2[k/k_d(\boldsymbol{x})]\}$ and larger $\eta(\boldsymbol{x})$ leads to smaller slope $\alpha_2(k_d/k_d(\boldsymbol{x})) < \alpha_2$. This explains the smaller values of slope observed in the DNS than in the curve given by theory. The dependency of the skewness S_2 on $\mathcal{R}_\lambda$ exists but is weaker than the effects of fluctuations in $k_d(\boldsymbol{x})$.

Let us consider the approximation in Eqs. (11)–(16). First, the Padé approximation in Eq. (11) is used to infer the approximate position of the pole of $F(\tilde{x})$ in the complex $\tilde{x}$ plane. In order to obtain a more precise position of the pole, we could proceed to the higher order terms in the Taylor expansion of $Q_{31}(\tilde{x})$ such as the term of $O(\tilde{x}^5)$. This would require knowledge of the higher order correlations such as $\langle \delta u_i(\boldsymbol{r})[\delta\omega(\boldsymbol{r})]^4\rangle$, $\langle(\partial u_1/\partial x)(\partial\omega/\partial x)^4\rangle$, and so on, which means that we would have to take into account the higher order correlations of vorticity and velocity fields. As the order of correction increased, the pole position would be corrected and approach more precise position, which would lead to a precise estimate of the slope of the energy spectrum in the far dissipation range. However, the inclusion of the higher order moments of vorticity and/or velocity is physically equivalent to taking into account the effects of intermittency on the slope or the pole position of $F(\tilde{x})$. We thus estimate that the order of the error associated with the Padé approximation is roughly of the order of the distance between the theoretical curve and the DNS values in Fig. 4. Second, the essential feature of the approximate form Eq. (16) is the exponent $(2-\delta)/2$, which leads to the exponent $-(3+\delta)/2$ in the prefactor of the energy spectrum in the dissipation range. From Fig. 3, we conclude that the matching form Eq. (16) is well supported, although more comparison at higher Reynolds numbers is necessary.

It is useful for understanding the universality of the energy spectrum to consider the relations among $\mathcal{R}_\lambda$, R_L, $l_d = 1/k_d$, λ and $L = 1/k_I$. Using Eqs. (26)–(29), we have

$$\frac{\lambda}{L} \sim R_L^{-1/2}, \quad \frac{l_d}{\lambda} \sim \mathcal{R}_\lambda^{-1/2}, \tag{42}$$

so that the ratio l_d/L becomes

$$\frac{l_d}{L} \sim (R_L \mathcal{R}_\lambda)^{-1/2}. \tag{43}$$

The microscale Reynolds number is

$$\mathcal{R}_\lambda = \frac{\Omega^{3/2}}{\eta} = \frac{\nu\Omega}{\eta}\frac{\Omega^{1/2}}{\nu} \sim \frac{\lambda^2}{L^2} R_L \sim R_L^0, \tag{44}$$

which means that $\mathcal{R}_\lambda$ is independent of R_L. We infer from the DNS data that this would occur at very high R_L. It is natural to assume that η is finite in the limit of vanishingly small viscosity, and the total enstrophy is conserved and finite in the inviscid limit when forcing is absent. From these two facts, it is quite reasonable to expect that the microscale Reynolds number $\mathcal{R}_\lambda$ approaches a nonzero finite value in the inviscid limit, although the limiting value is not known. If this statement is correct, the ratio l_d/λ becomes constant and l_d/L depends only on R_L. That is, R_L is the only dominant control parameter in the limit of vanishingly small viscosity. In this sense, our values of R_L are large but not enough to study the limit of constant $\mathcal{R}_\lambda$.

For finite R_L, it is observed from the DNS that the exponent δ in the inertial range decreases very slowly with R_L because it decays slowly with $\mathcal{R}_\lambda$. In this sense the spectrum in the inertial range is not universal. Similarly the exponential decay rate α_2 in the far dissipation range also decreases as $\mathcal{R}_\lambda^{-1/6}$, and thus it is not universal for finite R_L. However, when R_L becomes infinite, we can expect that δ vanishes and the spectrum in the inertial range tends to Eq. (1) which is dependent only on k_I. Also, α_2 becomes independent of $\mathcal{R}_\lambda$, so that we can consider that the energy spectrum in the far dissipation range tends to a universal form of exponential decay with the algebraic prefator $k^{-3/2}$. Although it is difficult to increase R_L even for the high performance computer, it is desirable and interesting to study the spectrum in both inertial and dissipation ranges at higher Reynolds numbers. Also, it is challenging to study whether or not the limiting value of $\mathcal{R}_\lambda$ exists and is universal.

ACKNOWLEDGMENTS

The author expresses his deep thanks to Mr. Hibino and Mr. Takahashi for their computational assistance. A discussion with Dr. Kraichnan is gratefully acknowledged.

APPENDIX

First we consider the one-dimensional enstrophy spectrum $W(k_1)$, which is computed as

$$W_1(k_1) = \int_{k_1}^{\infty} \frac{k^2 E(k)}{\sqrt{k^2 - k_1^2}}\, dk. \tag{A1}$$

Substituting Eq. (32) into this, we have

$$W_1(k_1)\approx C\eta^{2/3}k_d^{\delta}\int_{k_1}^{k_d}k^{-\delta}[\ln(k/k_I)]^{-\beta}\frac{dk}{k\sqrt{k^2-k_1^2}}$$
$$\approx C\eta^{2/3}k_d^{\delta}\left(\int_{k_1}^{ek_1}+\int_{ek_1}^{k_d}\right)k^{-\delta}[\ln(k/k_I)]^{-\beta}\frac{dk}{k\sqrt{k^2-k_1^2}}$$
$$\approx C\eta^{2/3}k_d^{\delta}(I_1+I_2). \tag{A2}$$

The integrals I_1 and I_2 are approximately evaluated for $k_1\gg k_I$ as follows:

$$I_1=\int_{k_1}^{ek_1}k^{-\delta}[\ln(k/k_I)]^{-\beta}\frac{dk}{k\sqrt{k^2-k_1^2}}$$
$$\approx k_1^{-(1+\delta)}[\ln(k_1/k_I)]^{-\beta}\int_{k_1}^{ek_1}\frac{dk}{\sqrt{k^2-k_1^2}}$$
$$\approx k_1^{-(1+\delta)}[\ln(k_1/k_I)]^{-\beta}\ln\left|\frac{ek_1^2+\sqrt{(ek_1)^2-1}}{k_1^2+\sqrt{k_1^2-1}}\right|$$
$$\sim k_1^{-(1+\delta)}[\ln(k_1/k_I)]^{-\beta}. \tag{A3}$$

In the integral I_2, the factor $1/\sqrt{k^2-k_1^2}$ is approximated as $1/k$ in the range of integration over k, so that

$$I_2=\int_{ek_1}^{k_d}k^{-\delta}[\ln(k/k_I)]^{-\beta}\frac{dk}{k\sqrt{k^2-k_1^2}}$$
$$\approx\int_{ek_1}^{k_d}k^{-(1+\delta)}[\ln(k/k_I)]^{-\beta}\frac{dk}{k}$$
$$\approx k_I^{-(1+\delta)}\int_{\ln(ek_1/k_I)}^{\ln(k_d/k_I)}e^{-(1+\delta)s}s^{-\beta}ds$$
$$\approx\frac{k_I^{-(1+\delta)}}{1+\delta}\left\{\left(\frac{ek_1}{k_I}\right)^{-(1+\delta)}[\ln(ek_1/k_I)]^{-\beta}-\left(\frac{k_d}{k_I}\right)^{-(1+\delta)}\right.$$
$$\left.\times[\ln(k_d/k_I)]^{-\beta}-\beta\int_{\ln(ek_1/k_I)}^{\ln(k_d/k_I)}e^{-(1+\delta)s}s^{-(1+\beta)}ds\right\}$$
$$\sim\frac{e^{-(1+\delta)}}{1+\delta}k_1^{-(1+\delta)}[\ln(ek_1/k_I)]^{-\beta}, \tag{A4}$$

to the leading order in $k_1/k_I\gg 1$, where integration by parts is used in the fourth line of Eq. (A4). Substituting Eqs. (A3) and (A4) into Eq. (A2), we obtain the asymptotic form of $W_1(k_1)$ as

$$W_1(k_1)\sim CB(\delta)\eta^{2/3}k_1^{-1}\left(\frac{k_1}{k_d}\right)^{-\delta}[\ln(k_1/k_I)]^{-\beta}, \tag{A5}$$

where

$$B(\delta)=1+\frac{e^{-(1+\delta)}}{1+\delta}. \tag{A6}$$

The function $F(\tilde{x})$ is given by the Fourier transform

$$F(x)=2\eta^{-2/3}Q_2(x_1)$$
$$=8\eta^{-2/3}\int_0^{\infty}W_1(k_1)[1-\cos(k_1x_1)]dk_1$$
$$\sim 8CB(\delta)k_d^{\delta}\int_{k_I}^{k_d}k_1^{-(1+\delta)}[\ln(k_1/k_I)]^{-\beta}$$
$$\times[1-\cos(k_1x_1)]dk_1$$
$$\sim 8CB(\delta)k_d^{\delta}\left(\int_{k_I}^{1/x_1}+\int_{1/x_1}^{k_d}\right)k_1^{-(1+\delta)}[\ln(k_1/k_I)]^{-\beta}$$
$$\times[1-\cos(k_1x_1)]dk_1$$
$$\sim 8CB(\delta)k_d^{\delta}(J_1+J_2). \tag{A7}$$

The two integrals J_1 and J_2 are approximated as follows:

$$J_1=\int_{k_I}^{1/x_1}k_1^{-(1+\delta)}[\ln(k_1/k_I)]^{-\beta}[1-\cos(k_1x_1)]dk_1$$
$$\approx\frac{x_1^2}{2}\left(\int_{k_I}^{ek_I}+\int_{ek_I}^{1/x_1}\right)k_1^{2-\delta}[\ln(k_1/k_I)]^{-\beta}\frac{dk_1}{k_1}$$
$$\approx\frac{x_1^2}{2}\left(k_I^{2-\delta}\int_{k_I}^{ek_I}[\ln(k_1/k_I)]^{-\beta}\frac{dk_1}{k_1}\right.$$
$$\left.+[\ln(k_{1*}/k_I)]^{-\beta}\int_{ek_I}^{1/x_1}k_1^{1-\delta}dk_1\right)$$
$$\sim\frac{1}{2(2-\delta)}x_1^{\delta}[\ln(k_{1*}/k_I)]^{-\beta},$$
$$ek_I<k_{1*}<1/x_1, \tag{A8}$$

and

$$J_2=\int_{1/x_1}^{k_d}k_1^{-(1+\delta)}[\ln(k_1/k_I)]^{-\beta}[1-\cos(k_1x_1)]dk_1$$
$$\approx\int_{1/x_1}^{k_d}k_1^{-(1+\delta)}[\ln(k_1/k_I)]^{-\beta}dk_1$$
$$\approx[\ln(k_{1**}/k_I)]^{-\beta}\int_{1/x_1}^{k_d}k_1^{-(1+\delta)}dk_1$$
$$\approx x_1^{\delta}[\ln(k_{1**}/k_I)]^{-\beta}[1-(k_dx_1)^{-\delta}]/\delta,$$
$$1/x_1<k_{1**}<k_d. \tag{A9}$$

Since the function $[\ln(k_1/k_I)]^{-\beta}$ with $\beta<1$ is a very slowly varing function of k_1/k_I, we can reasonably put $k_{1*}\sim 1/x_1\sim k_{1**}$ in Eqs. (A8) and (A9). When $1/x_1$ approaches k_d, J_2 becomes smaller than J_1. Then we obtain the asymptotic form of the function $F(\tilde{x})$ as

$$F(\tilde{x})\sim A(\delta)\tilde{x}^{\delta}\left[\ln\left(\frac{k_d}{k_I\tilde{x}}\right)\right]^{-\beta}, \tag{A10}$$

where $A(\delta)$ is given by

$$A(\delta)=\frac{4CB(\delta)}{2-\delta}. \tag{A11}$$

The total strain acting on the wave number k is computed as

$$\Omega_k = \int_{k_I}^{k} p^2 E(p)\,dp = C\eta^{2/3}\int_{k_I}^{k}\left(\frac{p}{k_d}\right)^{-\delta}[\ln(p/k_I)]^{-\beta}\frac{dp}{p}$$
$$= C\eta^{2/3}\left(\frac{k_d}{k_I}\right)^{-\delta}\delta^{\beta-1}\int_0^{\delta\ln(k/k_I)} e^{-t}t^{-\beta}dt$$
$$= C\eta^{2/3}\left(\frac{k_d}{k_I}\right)^{-\delta}\delta^{\beta-1}\gamma(1-\beta,\delta\ln(k/k_I))$$
$$\sim \frac{C}{1-\beta}\eta^{2/3}\left(\frac{k}{k_d}\right)^{-\delta}[\ln(k/k_I)]^{1-\beta}, \tag{A12}$$

where $\gamma(\mu,z)$ is the incomplete γ function.

[1] J. C. McWilliams, J. Fluid Mech. **146**, 21 (1984).
[2] M. E. Brachet, M. Meneguzzi, and P. L. Sulem, Phys. Rev. Lett. **57**, 683 (1986).
[3] B. Legras, P. Santangelo, and R. Benzi, Europhys. Lett. **5**, 37 (1988).
[4] M. E. Brachet, M. Meneguzzi, H. Politano, and P. L. Sulem, J. Fluid Mech. **194**, 333 (1988).
[5] P. Santangelo, R. Benzi, and B. Legras, Phys. Fluids **A1**, 1027 (1989).
[6] K. Ohkitani, Phys. Fluids **A2**, 1529 (1990).
[7] R. Benzi, G. Paradin, and A. Vulpiani, Phys. Rev. A **42**, 3654 (1990).
[8] M. E. Maltrud and G. K. Vallis, J. Fluid Mech. **228**, 321 (1991).
[9] M. E. Maltrud and G. K. Vallis, Phys. Fluids **A5**, 1760 (1993).
[10] V. Borue, Phys. Rev. Lett. **71**, 3967 (1993).
[11] Y. Hibino and T. Gotoh, Proc. RIMS **921**, 110 (1995).
[12] H. Takahashi and T. Gotoh, Proc. RIMS **972**, 163 (1996).
[13] R. H. Kraichnan, Phys. Rev. Lett. **72**, 1016 (1994).
[14] R. H. Kraichnan V. Yakhot, and S. Chen, Phys. Rev. Lett. **75**, 240 (1995).
[15] R. H. Kraichnan, Phys. Fluids **10**, 1417 (1967).
[16] C. E. Leith, Phys. Fluids **11**, 671 (1968).
[17] G. K. Batchelor, Phys. Fluids **12**, II-233 (1969).
[18] R. H. Kraichnan, J. Fluid Mech. **47**, 525 (1971).
[19] J. R. Herring, S. A. Orszag, R. H. Kraichnan, and D. G. Fox, J. Fluid Mech. **66**, 417 (1974).
[20] G.K. Batchelor, Cambridge Philos. Soc. **47**, 359 (1951).
[21] H. Effinger and S. Grossman, Z. Phys. **66**, 928 (1987).
[22] L. Shirovich, L. Smith, and V. Yakhot, Phys. Rev. Lett. **17**, 344 (1994); Errata, **20**, 1492 (1995).
[23] H. Tsuji, J. Phys. Soc. Jpn. **10**, 278 (1955).
[24] S. Chen, G. Doolen, J. R. Herring, R. H. Kraichnan, S. A. Orszag, and Z.-S. She, Phys. Rev. Lett. **70**, 3051 (1993).
[25] T. Tatsumi and S. Yanase, J. Fluid Mech. **110**, 475 (1981).
[26] Y. Kaneda, Phys. Fluids **A5**, 2835 (1993).
[27] G. Stolovitzky and K. R. Sreenivasan, Phys. Rev. E **52**, 3242 (1995).
[28] G. L. Eyink, Phys. Rev. Lett. **74**, 3800 (1995).
[29] A. Polyakov, Nucl. Phys. B **396**, 367 (1993).
[30] Y. Kaneda, Phys. Fluids **30**, 2672 (1987).